Macrothink Institute™

Journal of Biology and Life Science
ISSN 2157-6076
2026, Vol. 17, No. 2

The Digits of the Lizard *Podarcis muralis* Heal But Do Not Regenerate After Topical Application of Hyaluronate and FGFs

Alibardi Lorenzo

Dipartimento di Biologia, University of Bologna, via Semi 3, 40126, Bologna, Italy.
Email: lorenzo.alibardi@unibo.it

Received: March 9, 2026 Accepted: April 30, 2026 Published: June 30, 2026

doi:10.5296/jbls.v17i2.23884 URL: https://doi.org/10.5296/jbls.v17i2.23884

Abstract

Attempts to stimulate blastema formation and growth of digits in lizards have been carried out by topic treatments of a hyaluronate gel embedded with FGF1-2 on the amputated surface of digits. Six to ten topic coatings were applied on the stump surface during wound healing and after re-epithelialization, from 2 hours to 20 days post-amputation. Four lizards received injection of 5BrdU to evaluate cell proliferation. Histology of controls and treated digit stumps showed that a multilayered wound epidermis formed around 10-12 days post-amputation. Connective cells present underneath the wound epidermis gave rise to fibrocytes and numerous collagen fibrils after the second week post-amputation, turning the initial soft outgrowths of 0.3-0.5 mm into a solid and scaling scar at 32 days post-injury. Injection of 5BrdU revealed that cell proliferation was low in untreated and treated digit stumps at 12 and 32 days post-amputation, explaining the lack of growth of the initial digit outgrowth. The lack of regeneration may derive from limited penetration of hyaluronate-FGF. Cells activated on the stump surface are prevalently osteogenic, blocking digit regeneration. Next subcutaneous microinjections of hyaluronate-FGF gels might obtain a better stimulatory effect and induce formation of a growing digit outgrowth, as previously obtained for the limb.

Key words: lizard, digit, outgrowth, FGFs-hyaluronate treatment, microscopy

1. Introduction

While a variable healing of some tissues is present in terrestrial vertebrates, the ability to repair injury or loss of organs in amniotes (reptiles, birds and mammals), is limited and generally results in scarring (Ferguson & O'Kane, 1994; Carlson, 2005; Meenaski et al., 2005;

Beare et al., 2006; Jazwiska & Sallin, 2015; McCusker et al., 2015; Rinkevich et al., 2015; Alibardi, 2020a; Zaraisky et al., 2024). Recent analyses on the healing capability in amniotes, after the loss of total or parts of body appendages, have proposed a new evolutionary explanation for the loss of regeneration in amniotes (Alibardi, 2021, 2022, 2024a,b). Although the detailed molecular mechanisms remain to be discovered, the main problem to regenerate organs for terrestrial species is the dry or humid environment where they live. This environment is not permissive for regeneration but only for a rapid healing that generally leads to scarring (Ferguson & O'Kane, 1994). Only few amniotes are able to heal large tissues or partially some organs that have been damaged or largely removed by extended injuries during their lives, including appendages such as arms, legs or digits.

The regeneration of digits in urodele amphibians occurs by the formation of a small and soft embryonic-like organ termed the regenerative blastema that grows and reforms the lost phalanges (Smith, 1978). Digits and limb regeneration are rapidly lost in anuran tadpoles approaching metamorphosis, and this heteromorphic ability is completely lost in froglets (Dent, 1962). However, in juveniles metamorphosed within one month of the frog *Hyperolius viridiflavus*, digit regeneration has been documented, including the adhesive pad (Richards et al., 1975). No regeneration of digits occurs in adult reptiles (Bellairs & Bryant, 1968; Alibardi, 2020b), birds or mammals (Neufeld & Zhao, 1993; Zhao & Neufeld, 1995; Choi et al., 2017).

Two main examples of amniotes capable of large tissue recovery or heteromorphic regeneration are lizards among reptiles and spiny mice among mammals (Marcucci, 1930; Fisher et al., 2012; Gilbert et al., 2013; Lozito & Tuan, 2016; Alibardi, 2020a, 2021; Maden & Varholich, 2020). Lizards, aside the tail can also regenerate large cartilaginous tissues in the tail, limbs and vertebrae, while spiny mice regenerate large skin areas and, partially, some inner organs. Most lizard species can extensively regenerate their tail but no other appendages, such as limbs, arms or legs with their digits (Barber 1944; Bellairs & Bryant, 1968; Alibardi 2017a, 2021). The regenerated tail contains large groups of innervated segmented muscles, an axial cartilaginous cylinder surrounding the narrow spinal cord, large fat and connective tissues with nerves and blood vessels.

Previous studies showed that digits in lizards cannot regenerate after complete loss of the first or the second phalange (Bellairs & Bryant, 1968; Alibardi, 2020b). These studies have indicated that, after healing of the severed digit, a fibrotic connective tissue is formed on the digit stump at 2-3 weeks post-amputation, and this tissue produces a scar in 4-5 weeks. A regenerative process in lizards only occurs in the tail where a regenerative blastema is formed. The blastema grows to reform in a relatively short period, 1-2 months at warm temperatures, a simplified but however variably functional tail.

As part of a large survey on the ability of lizards to regenerate various tissues and organs, the present study was conducted on amputated digits under normal and experimental conditions, in the attempt to induce the formation of a regenerative blastema capable of growth. Similar attempts were previously done on the amputated limb, using FGFs embedded in a diluted hyaluronate solution (Alibardi, 2017b). Some studies have indicated that hyaluronate can

cross the mammalian skin, in both the epidermis and dermis, with a positive effect on the skin (Brown et al., 1999; Yang et al., 2012). Here, we have utilized a mix of FGFs and hyaluronate, indicated as healing solution, to stimulate digit regeneration in lizards. The present study deals with the fine description of the epidermal and dermal tissues formed on the digit tip of the wall lizard *Podarcis muralis*, after the application of the healing solution.

2. Materials and Methods

2.1 Animals and Experiments

In total, the digit tissues of twenty-eight adult wall lizards (*Podarcis muralis*), previously studied (Alibardi, 2020b), were again utilized in the present study. The reptiles were maintained in cages at 25-33ºC and they were fed with an insect diet, as previously reported (Alibardi, 2017b, 2020b). The procedures for care and handling the animals followed the Italian guidelines (Art. 5, DL 116/92). Initially, the lizards were maintained at 4ºC for about ten minutes to induce hypothermia, and the 4th or 5th digit was cut at about half of the second phalange. Twelve untreated healing digit stumps (controls) were collected and fixed at 3 days (n=1), 12 days (n=4), 18 days (n=3), 22 days (n=29), and 32 days (n=2) after amputation. Other eight lizards were instead treated with a "healing solution" made of 6% Sodium Hyaluronate (cat. 51770050, Acros Organic, New Jersey, USA) in Ringer solution, containing 20 ng/ l of a 1:1 mix of FGF1 and FGF2 (F5267 and SRP4038, Sigma-Aldrich, Saint Louis, MI, USA). This solution, containing FGFs, was previously utilized in a study on the induction of limb regeneration in lizards, based on previous information on the presence of FGFs in regenerating tail tissues (Alibardi, 2017b, 2021).

The treatments consisted in the application of the healing solution on the stump surface of the amputated and healing digits, in order to coat it forming a drop of this solution that was left in place over the stump surface for about 5 minutes before releasing the animal into the cage. After 12, 18 and 32 days from amputation, samples of the digits from the treated animals were collected and fixed. Treatments initiated at 2 hours after amputation, and were repeated every 2 days for 5 times in three animals, and tissue collection was done at 12 days post-amputation. Other three animals received eight treatments every 2 days, and tissues were collected at 18 days from amputation. Finally, other two lizards received 10 treatments every 2 days, and tissues were collected at 32 days post-amputation. After induced hypothermia, tissues were collected from the tip of the healing digits (about 1 mm) in controls and treated animals.

In order to study the distribution of proliferating cells, 4 lizards at 12 days (n=2 controls and n=2 treated) and other 4 lizards at 32 days (n= 2 controls and n=2 treated) post-amputation, were injected with 5BrdU in Ringer (dosage of 50 g/g Body weight), three hours before sampling. These eight lizards served for the immunofluorescence detection of 5BrdU-labeled cells, indicating cell proliferation in the collected tissues of control and treated animals. All the untreated and treated lizards (twenty), were returned to the wild after the experiment and only the eight lizards injected with 5BrdU were sacrificed.

2.2 Tissue Preparation and Microscopic Methods

Digit samples from treated and untreated animals were fixed for ten hours at 4 ºC in 5% formaldehyde in 0.2 M Phosphate buffer at pH 7.4, and they were dehydrated in ethanol until 90°, immersed in pure Bioacryl Resin for 3-4 hours, and exposed at 4ºC to UV light for 2 days in order to harden the resin (Scala et al., 1992). Tissues were sectioned at 2-4 m using an LKB-ultramicrotome, and some sections were stained with 1% Toluidine blue for the histological study. Other sections were instead utilized for immunohistochemistry, after collecting them on chromo-alum-albumin pre-coated slides that were dried on a hot plate at 40°C for some hours.

For blocking non-specific antigenic sites in the sections, a pre-incubation step of 30 minutes was done, immersing the sections in 0.05 M Tris Buffer at pH 7.4, with 5% of BSA and 2% NGS. The 5BrdU mouse antibody (G3G4), developed by SJ Kaufman, University of Illinois at Urbana-Champaign, USA, was purchased from the Hybridoma Bank of the University of Iowa, USA. The antibody was diluted 1: 50 (v:v) in buffer, and it was omitted in control sections. After incubation with the 5BrdU antibody overnight at 4°C, the sections were rinsed for 10 minutes with the buffer, and incubated for 1 hour at room temperature with a secondary anti-mouse antibody conjugated to FITC (Fluoresceine Thiocyanate, Sigma, USA) at 1: 200 v:v dilution. Sections were observed using a fluorescence microscope equipped with a Fluorescein filter, and images were recorded on a digital camera.

For electron microscopy, the tissues embedded in Resin Bioacryl were sectioned with an ultramicrotome, and thin sections of 50-90 nm in thickness were collected on Copper grids. They were dried and stained for forty minutes with 2% uranyl acetate, rinsed in distilled water, dried, and stained for eight minutes in 0.2% lead citrate in a lightly basic water solution, dried and then observed under a transmission electron microscope (Zeiss C10/CM), operating at 60 kV.

3. Results

3.1 Macroscopic Observations

After 7 days from the amputation, the untreated (control) stump of the digits formed a dry clot over the central phalangeal region, surrounded by a peripheral smooth surface, indicating partial re-epithelialization (Fig. 1 A). The treated stumps showed a smooth surface indicating complete re-epithelialization (Fig. 1 B). At 14 days post-amputation, both untreated and treated digit stumps were completely covered by a smooth epidermis and formed a soft 0.3-0.5 mm outgrowth, resembling a small regenerative blastema (Fig. 1 C). The phalangeal bone in the stump was no longer visible or formed a central small cavity (arrowhead in Fig. 1 D). At 21 days post-amputation, the blastema became harder and the wound epidermis was still shining in untreated and treated animals (Fig. 1 E, F). In some treated animals, the blastema showed an overgrown mass of tissue surrounding a small cavity corresponding to the central area where the phalangeal bone was present (arrowhead in Fig. 1 F). In both controls and in treated animals, no further growth occurred in the following days. At 32 days post-amputation, the blastema of 0.3-0.5 mm started to form scales in controls while it remained prevalently smooth but opaque in treated animals (Fig. 1 G, H).

3.2 Histology of Untreated (Controls) Samples

At three days post-amputation, the digits showed a damaged phalangeal bone, an exposed connective tissue, but no epidermis was observed over these tissues (Fig. 1 I). The distal most region of the bone showed an irregular periosteum formed by randomly distributed cells, possibly derived from periosteal degradation, cell proliferation or cell release. At 12 days post-amputation, the stump surface of untreated animals was completely repaired in those cases where no central phalangeal fragments were still present. The histological examination of untreated samples, showed a thicker wound epidermis than in the proximal scales, especially by the tip of the outgrowth close to the bone of the phalange (Fig. 1 J). Underneath the regenerating epidermis, a connective tissue formed by flat fibroblasts and sparse dermal melanophores was observed (Fig. 1 J). In the central area of the outgrowth, flat connective cells were more densely associated or even in continuation with the periosteum of the interrupted phalange.

At 18 days post-amputation, and in the following days, the outgrowth remained of the same length, about 0.3-0.5 mm, while a fibrous connective tissue, made of flat fibrocytes, occupied most of the outgrowth (Fig. 1 K). These cells were in continuity with the dermis or with some muscle fragments of the stump. The central mass of cells was in continuation with the periosteum of the phalangeal bone, and numerous cells were oriented around the phalangeal remnants, forming a sort of fibrous sheath (arrows in Fig. 1 K). Some darker areas located in front of the bone stump suggested that some mineralization was taking place among these cells, as later confirmed under electron microscopy (see later description).

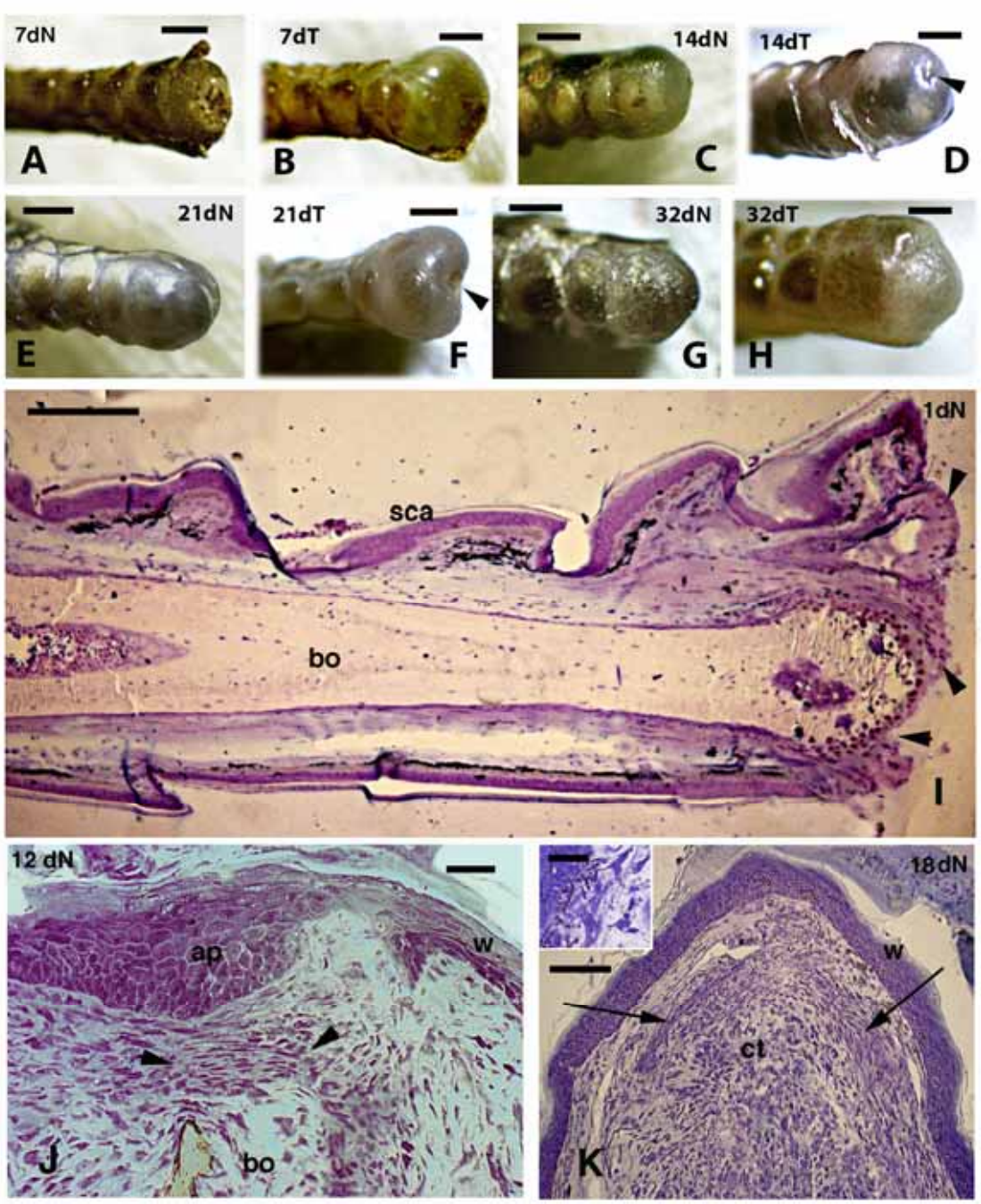

Fig. 1. Macroscopic aspect of amputated digits (N, normal untreated; T, treated) at progressive stages of recovering healing (**A-H**) and histological images (**I-K**, toluidine blue stain) of untreated digits. **A-B**, after 7 days; **C-D**, after 14 days; **E-F**, after 21 days; G-H, after 32 days; **A-H**, Bars, 0.5 mm. **I**, section of digit 1 day post-amputation (arrowheads indicates the stump surface) . Bar, 200 m. **J**, apical region of the digit stump at 12 days post-amputation showing the thick wound epidermis covering the inner connective tissue. A group of very flat fibrocytes (arrowheads) is interposed between the wound epidermis and the phalangeal bone. Bar, 20 m. **K**, at 18 days the digit tip is occupied by a dense irregular connective tissue beneath the wound epidermis. Arrows point to fibrous sheaths. Bar, 50 m. The inset (Bar, 10 m) shows the elongated fibroblasts in the outgrowth. **Legends**: ap, apical

epidermal peg; bo, bone (phalange); ct, connective tissue; sca, scales; w, wound epidermis (regenerating).

3.3 Histology of Treated Samples

Histological sections of treated digits at 12 days after amputation showed the formation of a thick wound epidermis covering the underlying connective tissue. The latter also formed a denser fibrous sheath in continuation with the phalangeal bone (Fig. 2 A, B). In some cases, a central epidermal peg, formed from numerous layers of keratinocytes, was seen at 12 days (Fig. 2 C, D). In other cases, where the distal bone of the phalange was still present on the digit surface, the regenerating epidermis formed multi-stratified epidermal pegs that penetrated underneath the bone, still surrounded by a fibrinous scab (Fig. 2 E). Higher magnification showed that the bone fragment contained numerous osteoclasts located between the bone and the migrating wound epidermis (Fig. 2 F). This condition indicated a discontinuity in the epithelial covering of the stump, and resembled the untreated digit stump at the same post-amputation time (Fig. 1 J; Alibardi, 2020b).

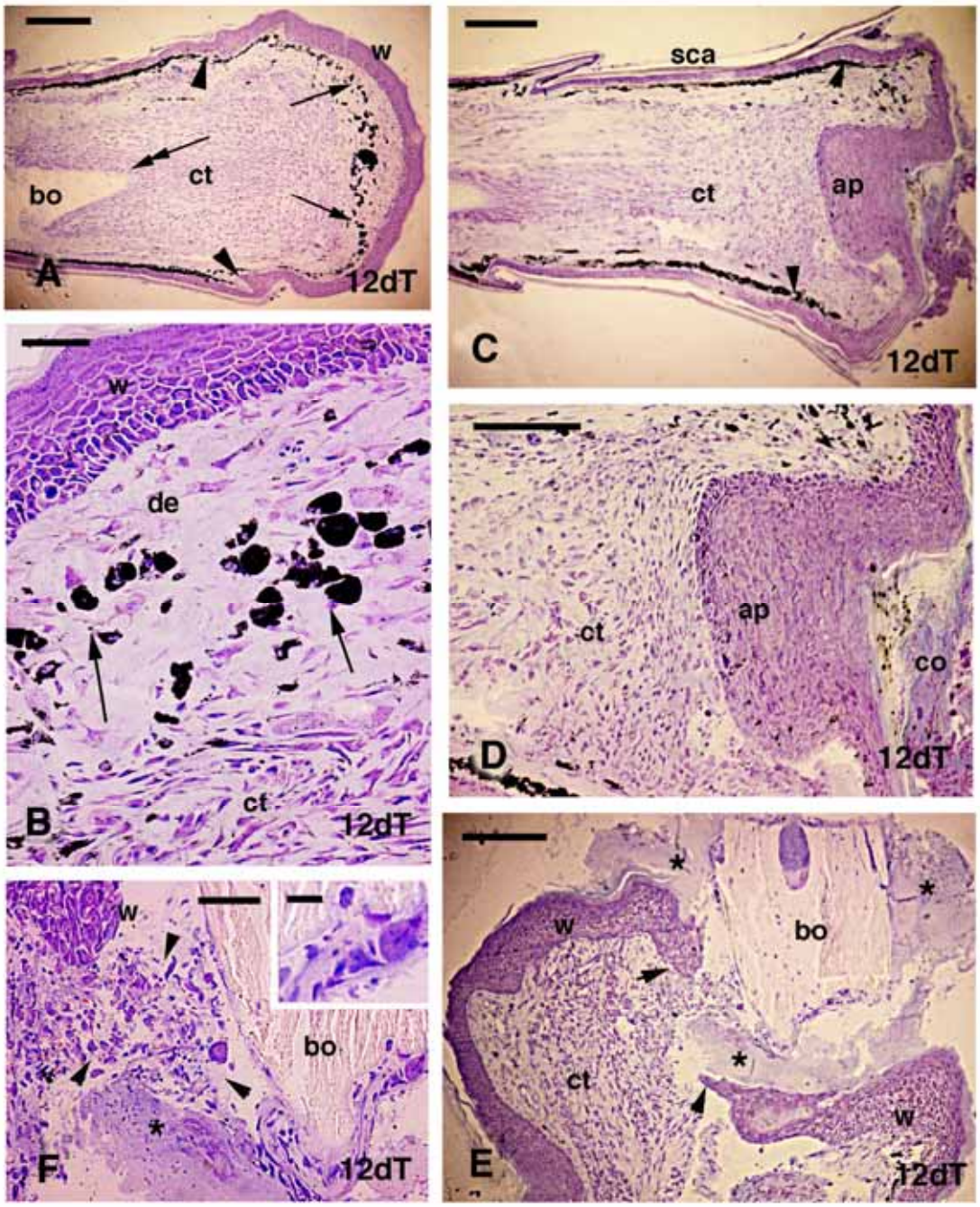

Fig. 2. Histological sections of treated (T) healing digits 12 days post-injection. Toluidine blue stain. **A**, low magnification view of a short outgrowth, evidencing the thicker wound epidermis in comparison to the epidermis of stump scales (arrowheads indicate the posterior limit of the outgrowth). A dense cellular region of the connective tissue is associated with the anterior part of the phalange remnant (double arrow) while the dermis, outlined by a melanophore line (arrows), appears of lower cell density. Bar, 100 m. **B**, higher magnification view of the apical dermis showing the thick wound epidermis, the numerous melanosomes (arrows) located in the superficial dermis that shows a lower cell density in comparison to the deeper connective tissue. Bar, 20 m. **C**, another digit stump with a short outgrowth (arrowheads indicate the posterior limit of the outgrowth), covered by a thick

wound apical epidermis peg. The central connective appears in continuation with the bone of the phalange (arrows). Bar, 100 m. **D**, detail of the apical epidermal peg contacted by free fibroblasts underneath. Bar, 50 m. **E**, section of an unclosed stump, and where a piece of phalangeal bone is still present on the surface of the stump. The two borders of the migrating wound epidermis (arrowheads) are seen under the bone and the fibrinous clot or scab (asterisks), so that the stump is not completely epithelialized. Bar, 50 m. **F**, detail of the boundary between bone and migrating wound epidermis. Free cells (arrowheads), including phagocytes and osteoclasts (inset, Bar, 10 m), are interposed between bone and connective cells and the fibrinous clot (asterisk). Bar, 20 m. **Legends**: ap, apical epidermal peg; bo, bone of the phalange; co, corneous layer; ct, dense connective tissue; de, dermis; w, wound epidermis

At 18 days post-amputation, numerous fibrocytes occupied the outgrowth, covered by a multi-layered wound epidermis. In two cases where the distal phalangeal bone was still present, it appeared degraded and eroded by numerous osteoclasts (Fig. 3 A, B). In treated digits, numerous azurophilic and roundish or more irregular small bodies, 5-10 m large, were seen underneath the thick wound epidermis and in continuation with the base of the excision bone and the superficial epidermis (arrows in Fig. 3 B). This detail suggested that these bodies represented fragments of the “healing solution” containing hyaluronate-FGFs, and that they were penetrated inside the connective tissue during the time of application of the healing solution. The connective tissue located beneath the wound epidermis was formed from flat fibrocytes, and showed a weak azurophilic extracellular dense matrix (Fig. 3 C).

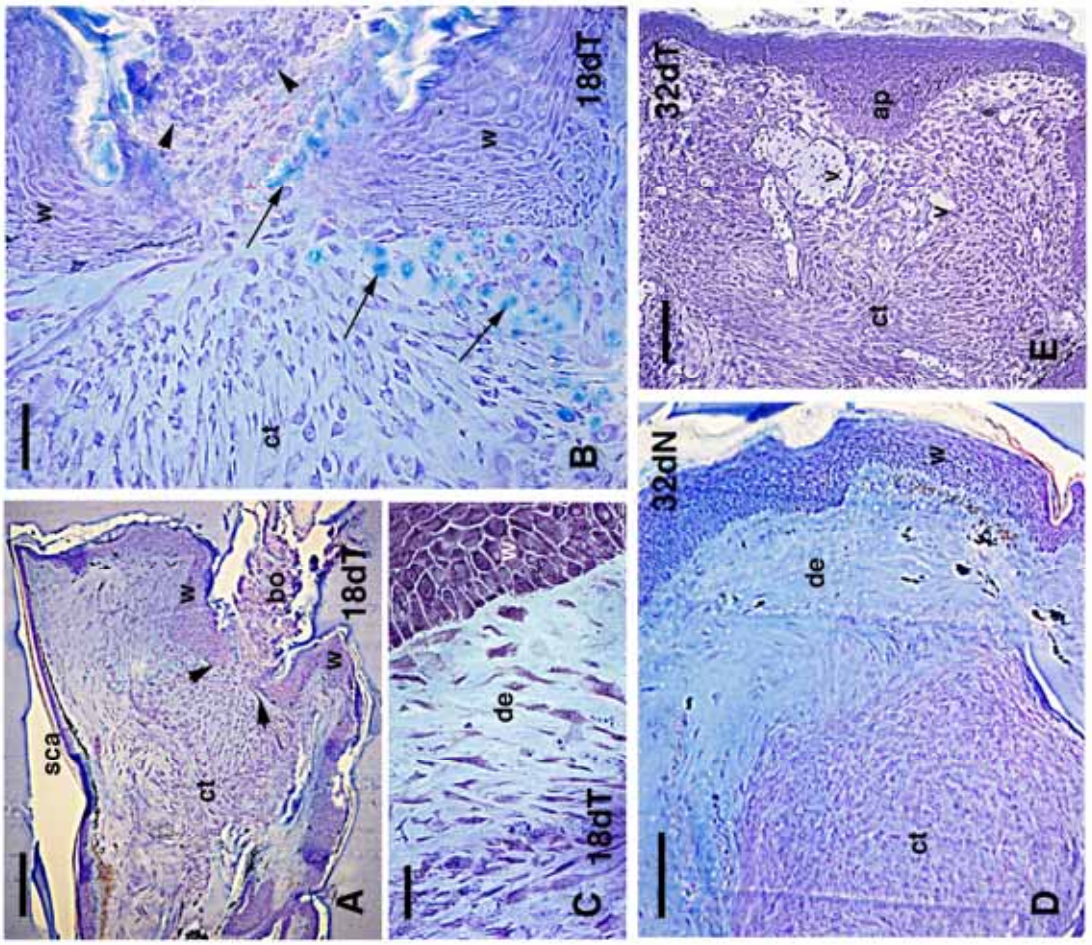

Fig. 3. Histological images of treated (T) and untreated normal (N) digits at 18 days (**A-C**) and 32 days (**D, E**) post-amputation. Toluidine blue stain. **A**, digit stump with remnants of the phalange bone that are still present on the surface at 18 days post-amputation. The wound epidermis forms two epithelial borders (arrowheads) underneath. Bar, 100 m. **B**, close-up to the previous image showing the eroded bone (arrowheads) and blue granules (arrows), indicating penetrated hyaluronate-FGFs gels from the outer epidermal surface. Bar, 20 m. **C**, detail of the dense dermis formed beneath the wound epidermis. Bar, 10 m. **D**, scarring outgrowth in an untreated (normal) digit stump at 32 days post-amputation. Bar, 50 m. **E**, dense and irregular connective tissue with enlarged blood vessels that have formed in a treated digit stump. Bar, 50 m. **Legends**: ap, apical epidermal peg; bo, bone remnant of a phalange going to be excised; ct, dense connective tissue; de, dermis (dense); sca, scale; v, blood vessels; w, wound epidermis.

At 32 days post-amputation, underneath the stratified wound epidermis a dense fibrous connective tissue, formed by sparse cells, was observed in untreated (Fig. 3 D) and treated samples (Figs. 3 E, 4). Sparse blood vessels were present among the irregular connective tissue. These outgrowths at 32 days post-amputation, showed two main histological aspects. In case the axial phalange was still present with its bony tissue, the latter was surrounded by a sheath of fibrous connective, likely representing a periosteum. The latter was neatly separated from an irregular dense connective tissue located underneath the wound epidermis (Fig. 4 A,

B). In other cases, the periosteum was not clearly delineated around a residual bone of the phalange. The bone was almost completely degraded, appearing as a fibrous connective rich in cells (Fig. 4 C, D). This homogenous dense connective tissue was formed from very flat fibrocytes with parallel orientation, immersed in a dense extracellular matrix (Fig. 4 D). Sparse dermal chromatophores were detected among fibrocytes, and some melanocytes were associated with the basal keratinocytes of the wound epidermis. Among osteocytes of the phalangeal bones, small areas occupied by neo-formed cartilaginous tissue were also noted (Fig. 4 A, C).

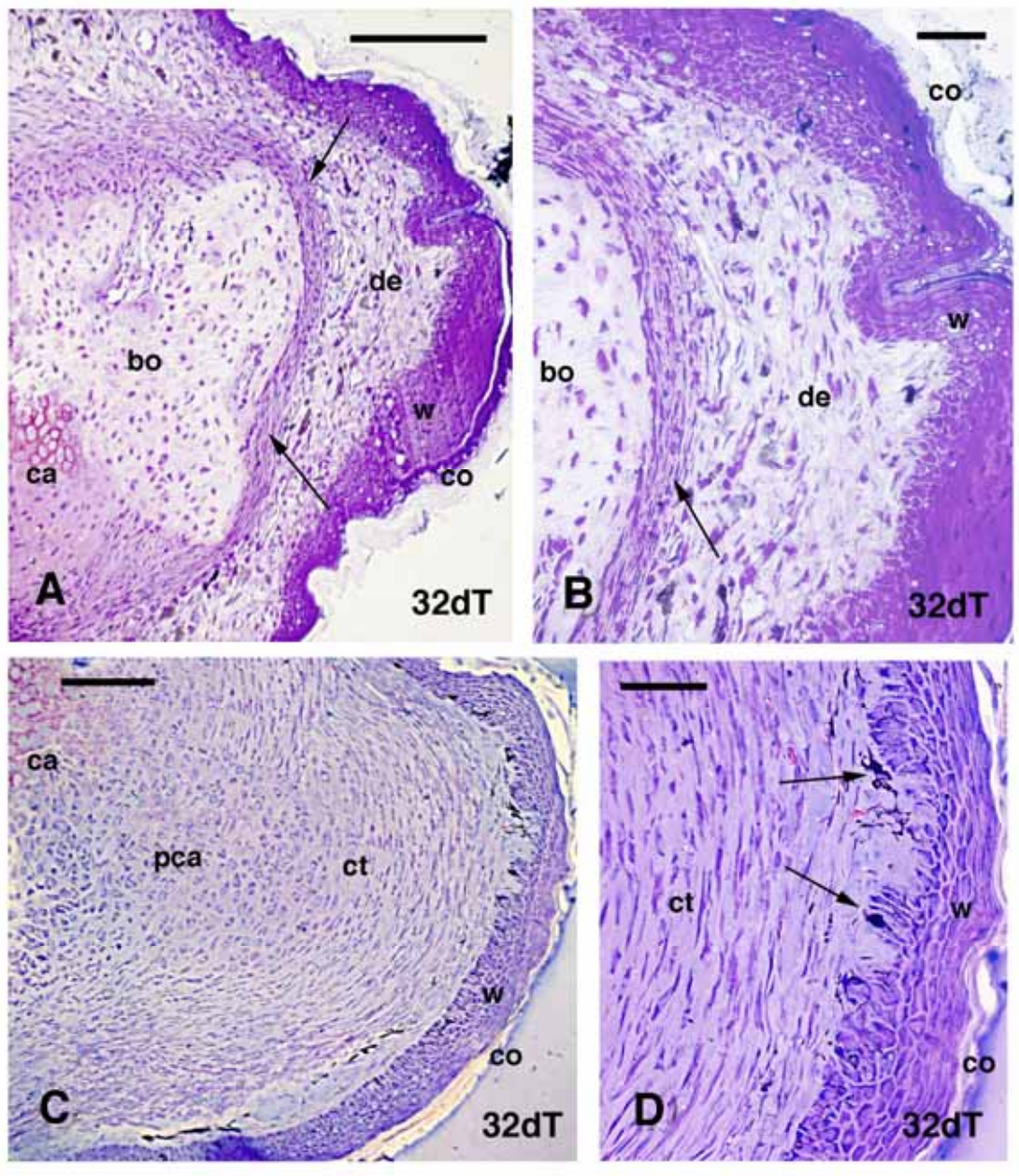

Fig. 4. scarring outgrowths of treated digit stumps (T) at 32 days post-amputation. **A**, only a thin dense dermis has been formed in front of the phalange bone, surrounded by a fibrous sheath, likely a periosteum (arrows). Bar, 100 m. **B**, close-up to the dense dermis of the

previous image, also showing a stratified epidermis. Bar, 20 m. **C**, in this case a dense apical connective tissue has formed in continuation with pre-cartilaginous and cartilaginous cells of the phalange. Bar, 50 m. **D**, higher view of the dense connective tissue composed from flat fibrocytes and dense extracellular matrix. Arrows point to melanocytes associated to the epidermis. Bar, 20 m. **Legends**: bo, phalangeal bone; ca, cartilage; co, corneous layer; de, dermis; pca, pre-cartilaginous cells; w, wound epidermis.

3.4 Immunolabeling for 5BrdU

The immunodetection of proliferating cells, using 5BrdU and FITC-immunofluorescence (green), showed sparse immunolabeled keratinocytes in basal and supra-basal layers of the wound epidermis. This observation was done for untreated and treated animals at 12 days after amputation (Fig. 5 A-D). Few sparse labeled cells, most likely fibroblasts, were also detected in the loose connective tissues forming the outgrowth at 12 days post-amputation. As indicate in Table 1, no quantitative difference in immunolabeled cells, was noted between two treated and two untreated lizards. Sparse labeled nuclei were also detected among muscles of the digit stump in the four cases (Fig. 5 D).

At 32 days post-amputation, the number of labeled cells generally decreased in comparison to the numbers of labeled cells observed at 12 days, especially in the wound (regenerating) epidermis. In the dermis, the number of labeled cells remained as low as after 12 days (Table 1). While some 5BrdU-labeled nuclei were still observed in the basal layers of the wound epidermis, rare labeled nuclei were detected in the dermis (Fig. 5 E-G). Table 1 also shows that no difference in the number of labeled nuclei was detected between treated and untreated lizards.

Table 1. Percentages of 5BrdU labeled cells (out of 900 total cells counted) found in outgrowths of untreated digits (= control healing digits, n = 2) with respect to the labeled cells present in treated digits (= using the healing solution, n = 2) at 12 and 32 days of regeneration. (* this counting includes all connective cells present beneath the wound epidermis in the healing digits in two lizards)

Time of healing	Wound epidermis	Connective tissue*
untreated 12days	2.9%	2.1%
untreated 12 days	2.5%	1.6%
treated 12 days	2.2%	2.1%
treated 12 days	2.4%	1.9%
untreated 32 days	0.9%	1.9%
untreated 32 days	1.3%	1.5%
treated 32 days	1.2%	1.9%
treated 32 days	1.4%	2.1%

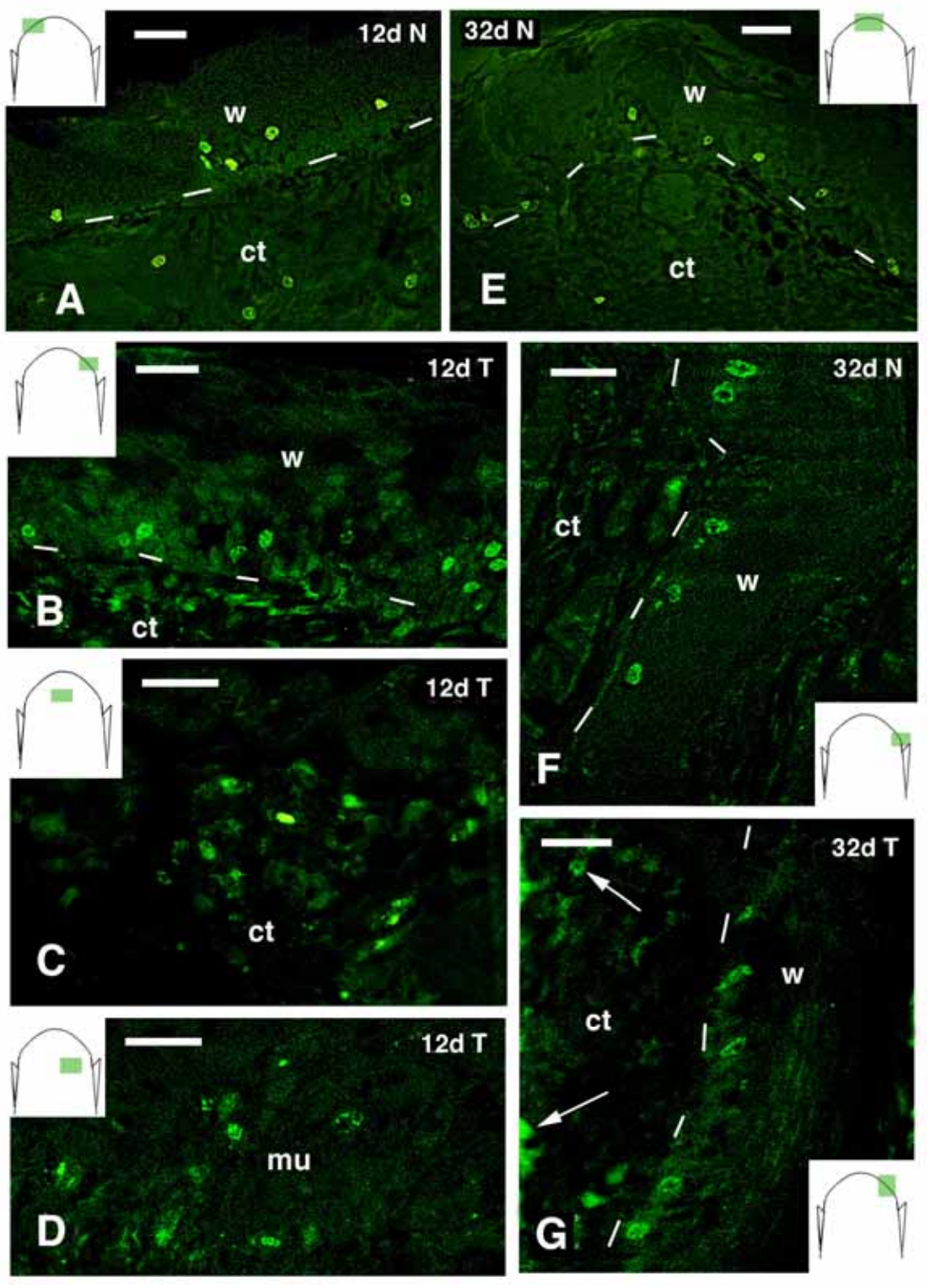

Fig. 5. FITC immunofluorescence of digit outgrowths at 12 and 32 days post-amputation, and 3 hours after 5BrdU injection (the associated drawings indicate the approximate area of localization of these cells in the digits). Bars in all figures, 10 m. **A**, apical wound epidermis of untreated normal digit (N) showing labeled nuclei (arrowheads) at 12 days post-amputation. Sparse labeled nuclei of fibroblasts are seen in the repairing connective tissue. **B**, detail of labeled cells localized in the basal layer of thick wound epidermis and

underlying dermis at 12 days from the amputation. **C**, a group of labeled likely fibroblasts detected in the central connective tissue of the stump. **D**, labeled nuclei within muscles of the digit stump at 12 days post-amputation. **E**, sparse labeled nuclei are still seen in the thick, apical wound epidermis at 32 days post-amputation. Rare labeled nuclei are detected in the fibrous connective tissue. **F**, labeled nuclei i-observed in the basal layer of the proximal, wound epidermis at 32 days. **G**, sparse labeled basal keratinocytes and fibroblasts (arrows) in the lateral epidermis. **Legends**: ct, connective tissue; mu, stump muscle; w, wound epidermis. Dashes underline the epidermis.

3.5 Electron Microscopy Study

Since no difference was detected between untreated and treated samples under light microscopy, electron microscopy observations were done on tissues from untreated samples. Also, although the quality of tissues fixed in formaldehyde could not be the same of tissues fixed with glutaraldehyde and osmium, the morphological details were however sufficient for the correct identification of cells and organelles.

The wound epidermis at 12 days post-injection appeared as a multi-stratified epithelium made of an irregular basal layer of flat keratinocytes, narrow supra-basal keratinocytes that accumulated lipid droplets and formed the stratum corneum (Fig. 6 A). Underneath the wound epidermis, the dermis was filled with collagen fibrils contacting an undulated basement membrane in which sparse elongated fibroblasts were present. On the surface of the phalangeal bones, some electron-dense cells, resembling macrophages, contacted an electron-pale fibrous matrix of collagen and granular material resembling an osteoid (Fig. 6 B). This material was probably little mineralized. Among the irregular-shaped fibroblasts, sparse multi-nucleated giant cells, likely osteoclasts, were commonly detected, close to the wound epidermis or to the phalangeal bones, as previously reported in the light microscopy description (Figs. 2F, 6 C; see Alibardi, 2020b).

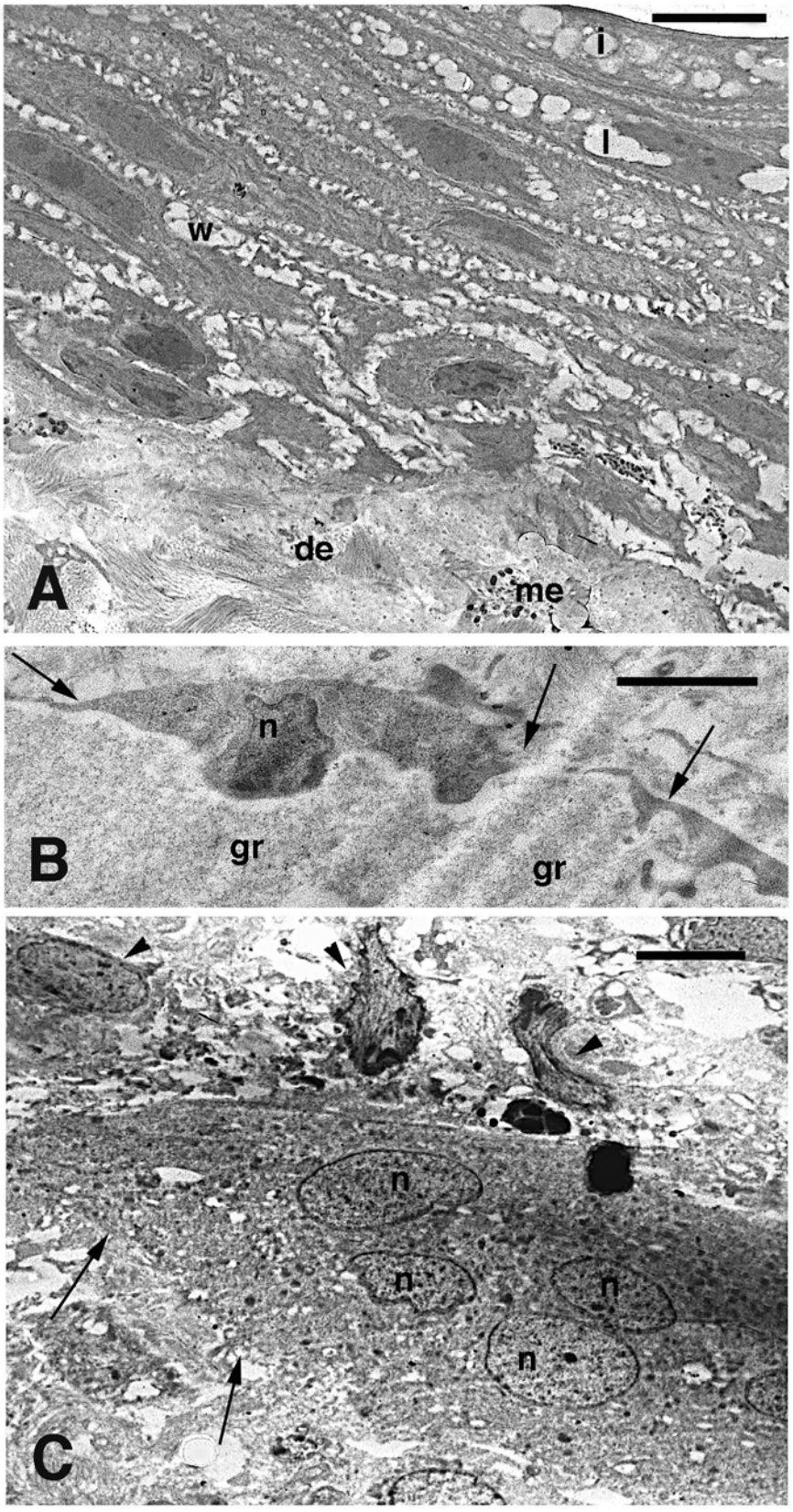

Fig. 6. Transmission electron microscopic images of regions of digit outgrowths at 12 days post-amputation. **A**, stratified wound epidermis, featuring a dense dermis and numerous lipid droplets accumulating in pre-corneous keratinocytes. Bar, 5 m. **B**, dark cells associated

(arrows) to a granular, possibly mineral matrix in the central phalange. Bar, 2 m. **C**, multinuclear large cell, likely an osteoclast, with irregular surface (arrows), located within the central connective tissue close to the bone of a terminal phalange. Arrowheads indicate possible phagocytes surrounding the osteoclast. Bar, 5 m. **Legends**: de, dermis; gr, granular extracellular matrix; l, lipid droplets; me, malanophore; n, nucleus; w, wound epidermis.

At 18 days post-amputation, the wound epidermis was formed from basal keratinocytes associated with an irregular basement membrane, and with the underlying, dense connective tissue forming the dermis (Fig. 7 A). The basement membrane was contacted by numerous collagen fibrils from the dermis. Numerous anchoring fibers, formed by collagen bundles, made frequent contacts with the basement membrane. The dermis contained a scarce number of cells that were immersed in a matrix containing banded collagen fibrils of type I, and that formed oriented parallel fascicles with the epidermis. In the dermis located by the apex of the outgrowth, sparse electron-dense fibrocytes were seen among an abundant collagenous matrix (Fig. 7 B). Sparse pale cells were in contact with the basement membrane of wound keratinocytes, and their cytoplasm was filled with 0.2-0.3 mm large round granules of low electron-density or containing internal lamellae. These cells were identified as the pterinosomes of xantophores. The plasma membrane appeared poorly preserved, rare ribosomes and sparse melanosomes were present in the cytoplasmic regions of these cells. Other cell organelles were rarely detected in these, possibly degenerating cells.

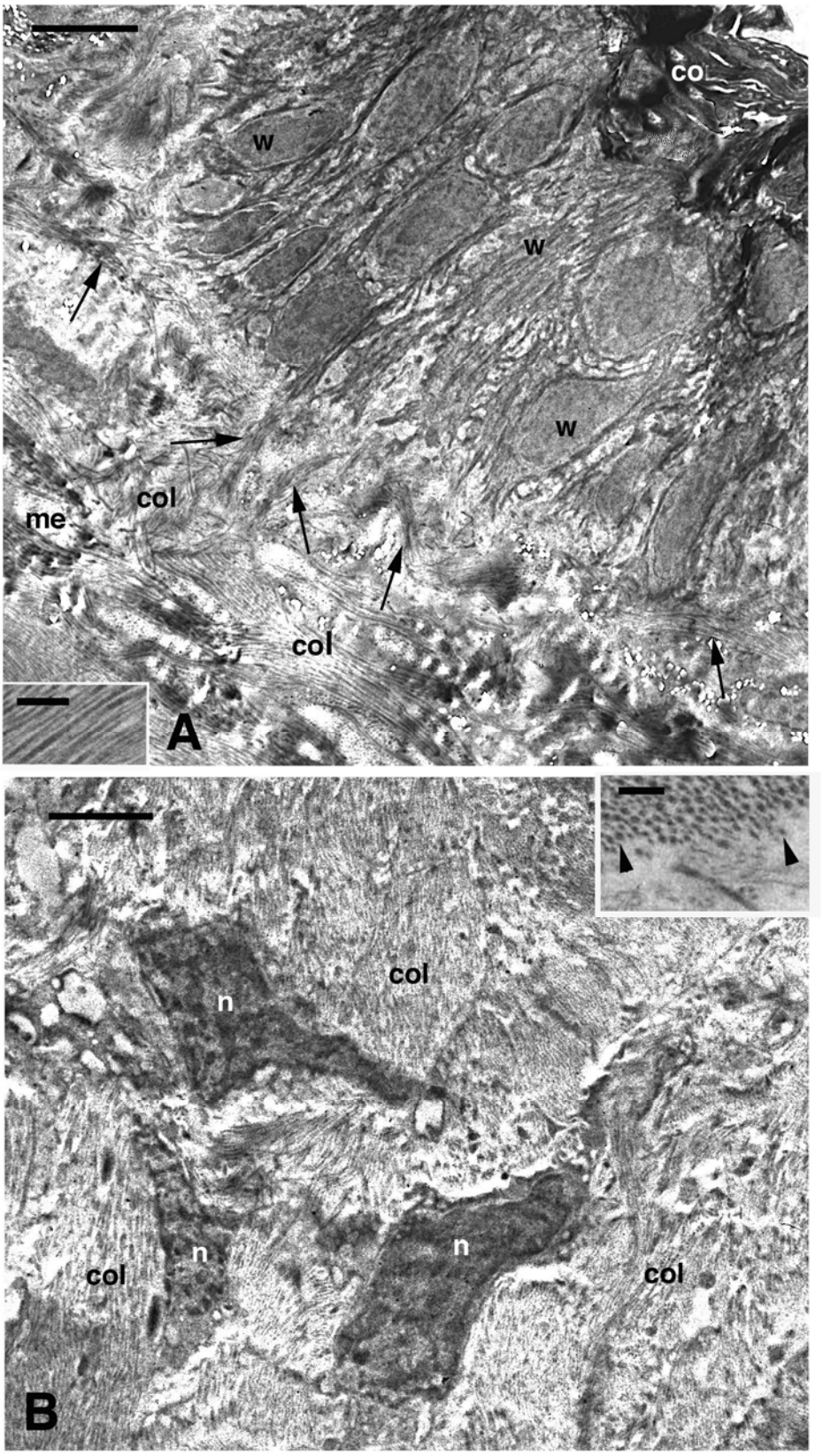

Fig. 7. Electron microscopy details of healing digits at 22 days post-amputation. **A**, a dense connective tissue rich in collagen fibrils and bundles is present underneath keratinocytes of the wound epidermis. Some collagen bundles (arrows) reach keratinocytes of the basal layer.

Bar, 5 m. The inset (Bar, 0.5 m) shows parallel collagen fibrils at higher magnification. **B**, three electron-dense fibroblasts completely surrounded by collagen fibrils in the central area of a digit outgrowth at 22 days. Bar, 2.5 m. The inset shows at higher magnification some collagen fibrils in cross section (arrowheads). Bar, 0.5 m. **Legends**: co, corneous layer of the wound epidermis; col, collagen bundles; me, melanophore; n, nucleus; w, wound epidermis.

At 22 days post-amputation, dark fibrocytes and melanophores were observed close to the phalangeal bone, and they appeared surrounded by a dense, collagen-rich extracellular matrix (Fig. 8 A). In the apical connective tissue present near the wound epidermis, other dark fibrocytes were embedded within a paler amorphous matrix. This was composed of a fine granulation, as observed at high magnification, resembling deposited extracellular fibrin (Figs. 3C, 8 B). Few thin cytoplasmic filopodes were seen along the perimeter of these “trapped” connective cells. The observation of the tissue area located in front of the severed phalange (refer position like in Fig. 4 A, B), showed numerous irregular-shaped and electron-dense fibrocytes that were in continuation with the periosteum surrounding the phalangeal bone (Fig. 9 A). In this region, the collagenous matrix contained electron-dense precipitates likely formed from calcium salts (Fig. 9 B and its inset). The dense precipitate was distributed over banded collagen type I fibrils. Also, at 32 days post-amputation the electron microscopic observations showed similar aspects in cells and extracellular matrix as those described at 22 days. A wound epidermis and its thick corneous layer were present, and the underlying tissues formed a scarring connective.

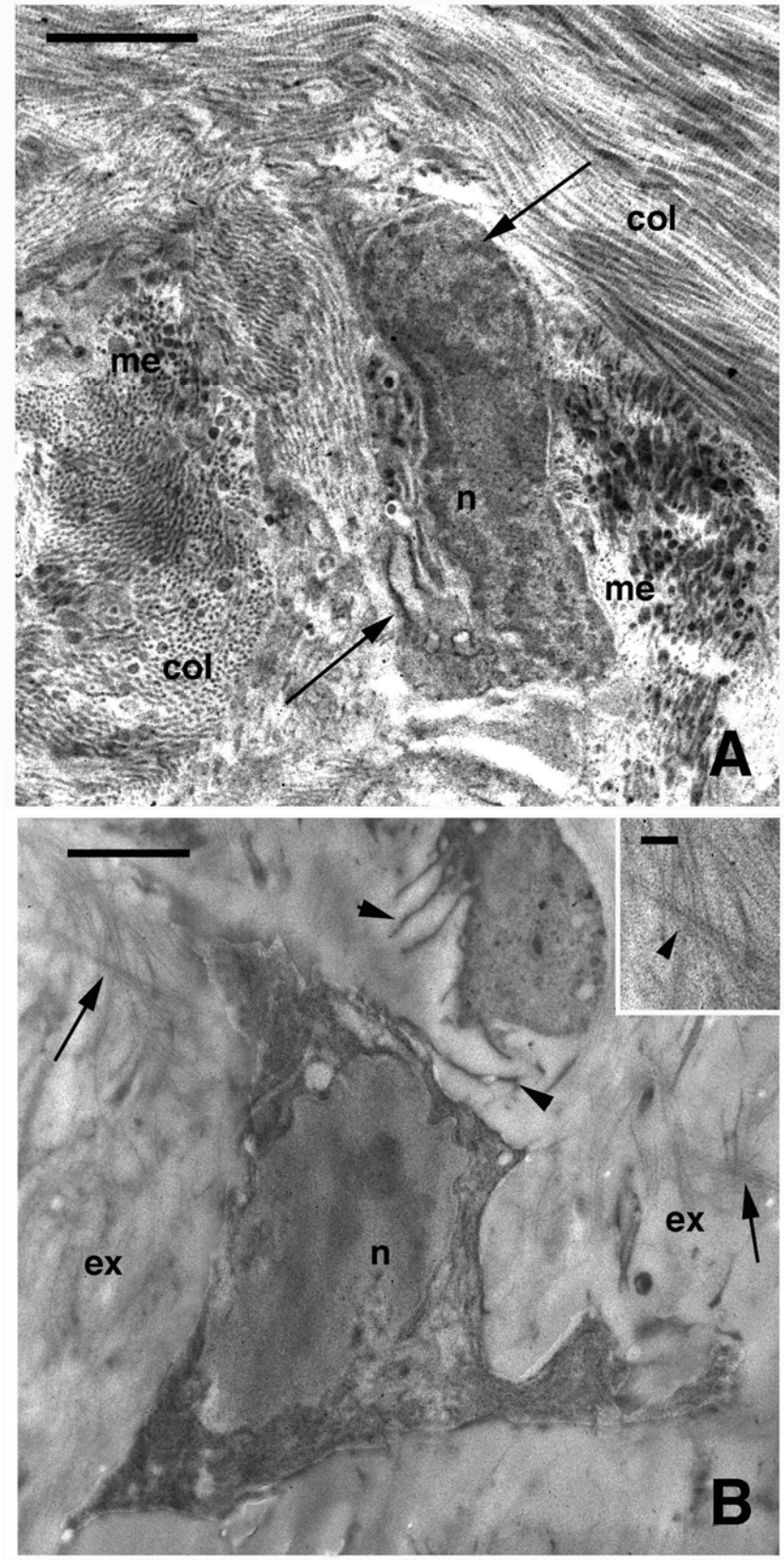

Fig. 8. Electron microscopy detail of the fibrotic connective tissue formed at 22 days post-amputation. **A**, likely dark melanophore (arrows) surrounded by a dense collagen matrix, located in the central region of the outgrowth, close to the phalange (referring position as in 1

J). Bar, 2 m. **B**, an electron-dense fibrocyte that appears embedded within an electron-pale, finely granulated extracellular matrix. This cell shows few thin filopodia (arrowheads) entering the matrix where sparse collagen fibrils (arrows) are present. Bar, 2 m. The inset (Bar, 400 nm) details these fibrils (arrowhead) that are immersed within a pale granulated matrix (fibrin-like). **Legends**: col, collagen fibrils (longitudinal- or cross-sectioned); ex, extracellular matrix; me, melanophore cytoplasm; n, nucleus; w, wound epidermis.

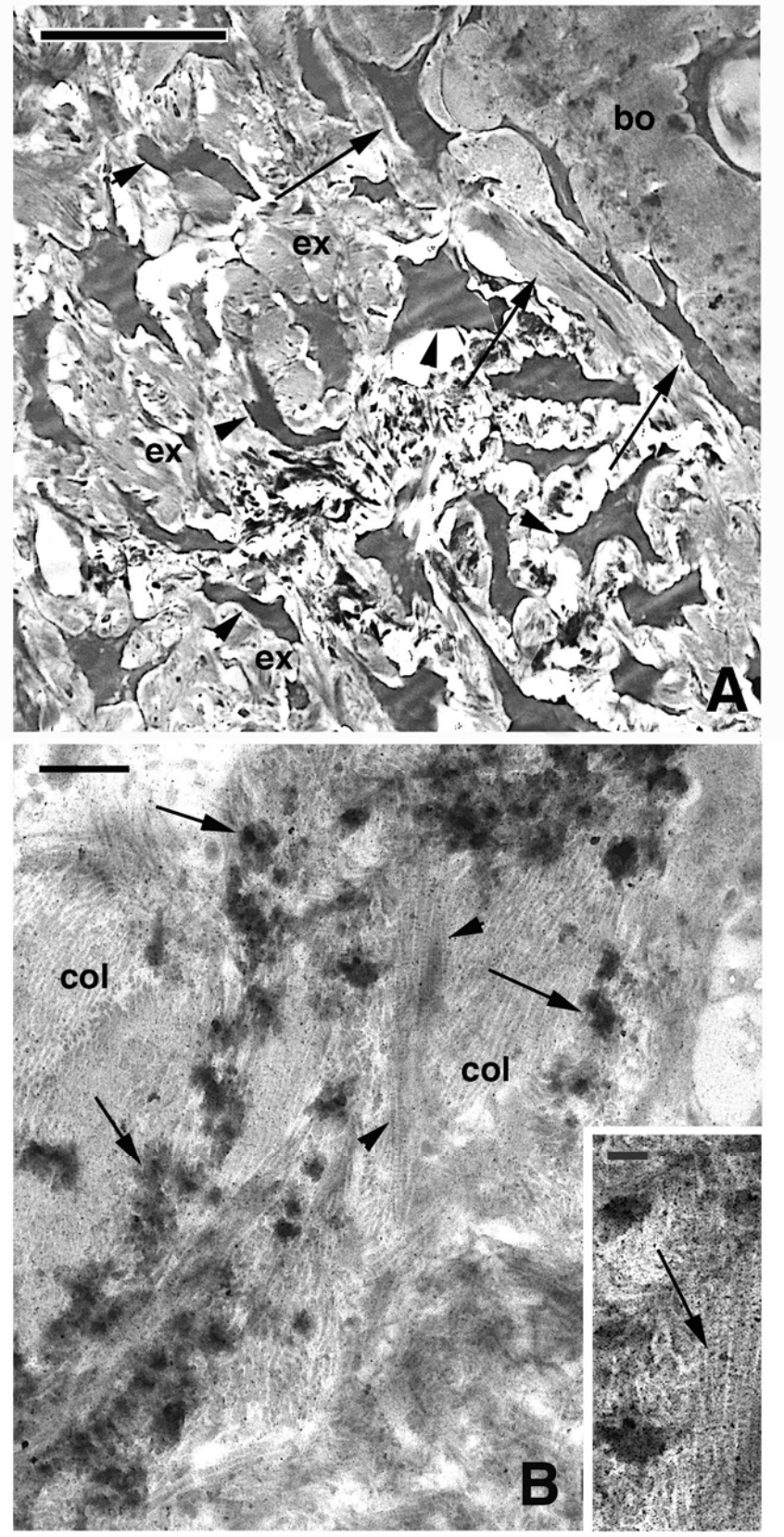

Fig. 9. Electron microscopy views of a small region within the central fibrotic connective tissue close to the phalangeal bone, in a digit stump at 22 days post-amputation. **A**, boundary region between the bone and the surrounding layer of flat cells (arrows), likely representing a

periosteum layer. Numerous irregular and electron-dense cells (arrowheads), likely osteogenic, are present in continuation with the periosteum. Bar, 10 m. **B**, detail of the extracellular matrix enriched in collagen fibrils that is present in front of the phalangeal bone. Numerous collagen fibrils appear associated with electron-dense nuclei of likely calcium deposition (arrows). Bar, 1 m. The inset (Bar, 200 nm) shows that the electron-dense deposits contact the banded collagen fibrils (arrowhead). **Legends**: bo, bone matrix; col, collagen fibrils; ex, extracellular matrix; n, nucleus.

4. Discussion

4.1 Digit Healing After GFs Treatments

The present study has utilized FGF1-2 incorporated within a hyaluronate gel and its goal was to stimulate the formation of a larger digit outgrowths in comparison to un-treaded animals. The study aimed to evaluate whether this gel could penetrate across the open wound during the first week post-amputation, and also through the regenerating epidermis formed after 2 weeks. Because of the small size of lizard digits, injections of the FGF-hyaluronate solution into the healing digit stump of 0.3-0.5 mm were not done (Fig. 1 C or D). Unfortunately, we did not have the technical ability to make microinjections of the “healing solution” in the small outgrowths. Therefore, only the exposed stump surface during the healing process was available for the penetration of the healing solution. Despite this limitation, it was tested whether a topical application to the surface of the stump during healing and in the following re-epithelialization, could stimulate digit regeneration. A penetration throughout the epidermis of mice was previously indicated using only hyaluronate or hyaluronate coupled with growth hormone, which showed a penetration through the skin in 30-60 minutes (Brown et al., 1999; Yang et al., 2012).

In lizards kept at 25-28°C, skin re-epithelialization of 3-6 mm large wounds in the trunk takes 7-8 days, and 8-14 days in the tail after autotomy, (Gilbert et al., 2013; Wu et al., 2014; Alibardi, 2017a, 2021). The complete digit re-epithelialization takes 7-12 days, so that direct penetration of the "healing solution" occurs only during this limited period (Alibardi, 2017a). This is also suggested from the histological study where the penetration of hyaluronate-containing material is indicated from the presence of "blue granules" (arrows in Fig. 3 B). Over half of the digits within 2-3 weeks of treatment (8 versus 6 cases observed) showed an overgrowth effect, suggesting that the growth stimulation derived from the penetration of the healing solution into the tissues of the treated digit stump (Fig. 1 D, F). The presence of overgrown tissues peripherally in comparison to the central region occupied by the phalanges at 14-22 days post-amputation in the treated animals (Figs. 1F, 3 A, B), suggests that during the first days from amputation some permeation of the "healing solution" took place. This could indeed have stimulated tissue regeneration.

This result was obtained when there was a delay in epidermal closure around the remnants of the distal phalange, before cleaving the bone fragments from the surface of the digit stump (Fig. 3 A, B). Later, the completion of a corneous layer over the wound epidermis blocked the penetration of the healing solution into the underlying connective tissue. The present study therefore suggests that, differently from mammalian epidermis (Brown et al., 1999; Yang et al., 2012), the wound epidermis formed in lizard digits is relatively impermeable to gels

vehicles containing hyaluronate. It is unknown whether the treatments here utilized accelerated the re-epithelialization but, despite the initial difference between untreated and treated digits, both eventually formed scars. Also, the number of 5BrdU-labeled cells was similar between untreated controls and treated animals (Table 1), and proliferation was even lower than in the scarring limb (Alibardi, 2017a). Previous experiments on amputated and larger limbs in lizards, injected with the vehicle and FGFs, stimulated the production of outgrowths that reached 3-4 mm in length, before scaling (Alibardi, 2017b). In those cases, it was possible the injection of the healing solution inside the forming outgrowths. Therefore, only an internal tissue delivery of FGFs or other growth factors through microsurgery appears to stimulate some growth in the amputated digits.

4.2 Scarring of Amputated Digits in Amniotes

The intense inflammation that follows digit amputation, determines the deposition of large masses of collagen fibrils, prevalently of type I. Due to the smaller size of fingers in comparison to the limb, and the relatively abundant area occupied from the phalangeal bone and its periosteum on the stump surface, the digital outgrowth is likely mainly made from osteogenic cells. The latter deposit high level of collagen I and, later, also of calcium salts in the extracellular matrix. This leads to the formation, within 22-32 days from the amputation, of a central outgrowth of mineralized fibrous connective tissue that hampers further digit regeneration. Although the final outcome of the present study was not successful, it allowed evaluating how to conduct possible treatments using a hyaluronate-based vehicle to deliver growth factors or signaling molecules to amputated appendages in reptiles.

Organ regeneration involves re-patterning of the regenerating structure and is present only in various invertebrates and in numerous fish and amphibians among vertebrates (Carlson, 2005; Kawakami, 2010; McCusker et al., 2015; Durant & Whited, 2021; Alibardi 2024a,b). Every wound or the amputation of an organ in amniotes, induces a strong inflammatory reaction that initially triggers numerous mast cells and granulocytes. Later, macrophages and lymphocytes arrive in the wounded area, and tend to remain among the granulation tissue addressing the healing process toward scarring (Meenaski et al., 2005; Mescher & Neff, 2006; Gourevitch et al., 2008; Fernando et al., 2011; Mescher et al., 2016; Choi et al., 2017; Alibardi, 2020b; Durant & Whited, 2021).

The injury of a limb or digits triggers the differentiation of fibrocytes underneath the thick wound epidermis (Barber 1944; Bellairs & Bryant, 1968; Alibardi, 2020b). Also, repairing transected bones can originate cartilaginous tissues in lizards (Pritchard & Ruzicka, 1950; Alibardi, 2021). This process stops any further growth of the digit, leading to small or large hypertrophic scars as in mammals and humans (Neufeld & Zhao, 1993; Zhao & Neufeld, 1995; Meenaski et al., 2005; Jazwiska & Sallin, 2015). Cell proliferation is low in the regenerating digit epidermis, and even lower in the connective, bony and other tissues of the digit stump at 12-32 days post-amputation, blocking the elongation of digit outgrowths (Alibardi, 2017a, 2020b).

Studies of the last 10-15 years consider the immune cell rejection among the main responsible cause of the regenerative failure in vertebrates (Mescher & Neff, 2006; Mescher

et al., 2016; Godwin & Rosenthal, 2014; Alibardi, 2020a, 2021; Aztekin & Storer, 2021). This likely occurs from the elimination of embryonic-like antigens formed on the cell surface of mesenchymal and epithelial cells, antigens no longer recognized as self from the definitive lymphocytes of the adult body. Fibroblasts are present in adult tissues, and the proliferation of these cells is tolerated by immune cells, but these cells determine a massive deposition of collagen and other dense extracellular proteins that form a scarring tissue.

In case of mammals, some limb and digit "regeneration" is reported to occur in early rat embryonic stages (Deuchar, 1976), in rat newborns (Scharf, 1961), and in the developing or fetal opossum (Mizell, 1968; Mizell and Isaacs, 1970). Other studies indicated that the distal half of the last phalange can "regenerate" in juveniles of mice and humans (Douglas, 1972; Illingworth, 1974; Choi et al., 2017; Schultz et al., 2018). The above cases, indicated as "regeneration", represent a recovering healing that gives rise to a minute part of the digit outgrowth, of less than 0.5 mm in mice or 1-3 mm in human. This outgrowth is associated with the germinal zone of the claw or nail, organs that are in a continuous growth and/or remodeling in these mammals. Digit healing takes place during somatic growth in mice and in children, and the relative contribution of regenerating cells or of the growth plates of phalanges that are actively producing new cells for the somatic growth of these mammals is undetermined. The minute elongation of the fingertips in mice and children is derived from the physiological elongation of the bone of fingers during their natural growth, a process that includes also the growth of the damaged fingertip. Rarely the length of the lost digit reaches the normal length of un-amputated digits in humans and the elongation of these fingers is largely due to somatic growth during the years of growth of the child into an adult. This healing process, a super-imposed somatic growth or remodeling in embryos or juveniles together "regeneration" after digit loss, is indicated more properly as *regengrow*, namely *regen*eration together somatic *grow*th (Alibardi & Meyer-Rochow, 2021; Alibardi, 2022, 2024a.b).

In conclusion, the present study confirms that digit regeneration does not occur in normal or experimental conditions in lizards, as previously seen (Bellairs & Bryant, 1968; Alibardi, 2020b). The failure of digit regeneration in lizards occurs with similar histological aspects as for those of mammals (Neufeld & Zhao, 1993; Zhao & Neufeld, 1995; Gourevitch et al., 2008; Fernando et al., 2011; Choi et al., 2017).

Acknowledgments

Study supported through Comparative Histolab Padova, Italy.

Author contributions

Not applicable.

Funding

Not applicable.

Competing interests

No conflicts of interest are present in this manuscript.

Informed consent

Obtained.

Ethics approval

The Publication Ethics Committee of the Macrothink Institute.

The journal's policies adhere to the Core Practices established by the Committee on Publication Ethics (COPE).

Provenance and peer review

Not commissioned; externally double-blind peer reviewed.

Data availability statement

The data that support the findings of this study are available on request from the corresponding author. The data are not publicly available due to privacy or ethical restrictions.

Data sharing statement

No additional data are available.

Open access

Copyrights

References

Alibardi, L. (2017a). Cell proliferation in the amputated limb of lizard leading to scarring is reduced compared to the regenerating tail. *Acta Zoologica, 98*, 170-180.

Alibardi, L. (2017b). FGFs treatments on amputated limbs stimulate the regeneration of long bones, opening new avenues for limb regeneration in amniotes. A morphological study. *Journal of Morphological and Physiological Kinesiology, 3*, 25.

Alibardi, L. (2020a). Appendage regeneration in anamniotes utilizes genes active during larval-metamorphic stages that have been lost or altered in amniotes: the case for studying lizard tail regeneration. *Journal of Morphology, 281*, 1358-1381.

Alibardi, L. (2020b). Microscopic observations on amputated and scarring lizard digits show an intense inflammatory reaction. *Zoology, 139*, 125737.

Alibardi, L. (2021). Review. Tail regeneration in lepidosauria as an exception to the generalized lack of organ regeneration in amniotes. *Journal of Experimental Zoology, 336B*,

145-164.

Alibardi, L. (2022). Regeneration in anamniotes was replaced by regengrow and scarring in amniotes after land colonization and the evolution of terrestrial biological cycles. *Developmental Dynamics, 251*, 1404-1413.

Alibardi, L. (2024a). Regeneration and regengrow in multicellular animals derive from the presence of processes of organ metamorphosis and continuous growth in their life cycles. *Acta Zoologica 105*, doi 10.1111/azo.12487.

Alibardi, L. (2024b). Speculations on the loss of regeneration derived from developmental modifications during land adaptation in some evolutionary lineages of animals. *Acta Zooologica,* doi.org/10.1111/azo.12498.

Alibardi, L., & Meyer-Rochow, V. B. (2021). Regeneration in Reptiles Generally and the New Zealand Tuatara in Particular as a Model to Analyze Organ Regrowth in Amniotes. *Journal of Developmental Biology 9*, 36.

Aztekin, C., & Sorer, M. A. (2021). To regenerate or not regenerate: vertebrate model organisms of regeneration-competency and -incompetency. *Wound Repair and Regeneration, 30*, 623-635.

Barber, L. W. (1944). Correlations between wound healing and regener- ation in fore-limbs and tails of lizards. *Anatomical Record, 89*, 441–453.

Beare, A. H. M., Metcalfe, A. D., & Ferguson, M. W. J. (2006). Location of injury influences the mechanisms of both regeneration and repair within the MRL/MpJ mouse. *Journal of Anatomy, 209*, 547-559.

Bellairs, A.d'A., & Bryant, S. V. (1968). Effects of amputation of limbs and digits of lacertid lizards. *Anatomical Record, 161*, 489-496.

Brown, T. J., Alcorn, D., & Fraser, R. E. (1999). Absorption of hyaluronan applied to the surface of intact skin. *Journal of Investigative Dermatology, 113*, 740-746.

Carlson, B.M. (2005). Some principles of regeneration in mammalian systems. *Anatomical Record, 287B*, 4-13.

Choi, Y., Meng, F., Cox, C.S., Lally, K. P., Huard, J., & Li, Y. (2017). Regeneration and regrowth potentials of digit tips in amphibians and mammals. *International Journal of Cell Biology,* doi.org/10.1155/2017/5312951.

Dent, J. N. (1962). Limb regeneration in larvae and metamorphosing individuals of the South African clawed toad. *Journal of Morphology, 110*, 61–79.

Deuchar, E. M. (1976). Regeneration of amputated limb-buds in early rat embryos. *Journal of Embryology and Experimental Morphology* 35, 345-354.

Douglas, B. S. (1972). Conservative management of guillotine amputation of finger in children. *Australian Paediatric Journal, 8*, 86-89.

Durant, F., & Whited, J. L. (2021). Finding solutions for fibrosis: understanding the innate mechanisms used by super-regenerator vertebrates to combat scarring. *Advanced Science, 8*, 2100407.

Ferguson, M. W. J., & O'Kane. S. (2004). Scar-free healing: from embryonic mechanisms to adult therapeutic intervention. *Philosophical Transactions of the Royal Society of London, 359B*, 839–850.

Fernando, W. A., Leiniger, E., Simkin, J., Carrie, L, Malcom, C. A., Sathyamoorthi, S., … & Muneoka, K. (2011). Wound healing and blastema formation in regenerating digit tips of adult mice. *Developmental Biology, 350*, 301-310.

Fisher, R. E., Geiger, L. A., Stroik, L. K., Hutchins, E. D., George, R. M., DeNardo, D. F., … & Wilson-Rawls, J. (2012). A histological comparison of the original and regenerated tail in the green anole, *Anolis carolinensis*. *Anatomical Record, 295*, 1609-1619.

Gilbert, E. A. B., Payne, S. L., & Vickaryous, M. K. (2013). The anatomy and histology of caudal autotomy and regeneration in lizards. *Physiological and Biochemical Zoology, 86*, 631-644.

Godwin, J. W., & Rosenthal, N. (2014). Scar-free wound healing and regeneration in amphibians: immunological influences on regenerative success. *Differentiation, 87*, 66-75.

Gourevitch, D. L., Clark, L., Bedelbaeva, K., Leferovich, J., & Heber-Katz, E. (2009). Dynamic changes after murine digit amputation: the MRL mouse digit shows waves of tissue remodeling, growth, and apoptosis. *Wound Repair and Regeneration, 17*, 447-455.

Illingworth, C. M. (1974). Trapped fingers and amputated finger tips in children. *Journal of Pediatric Surgery, 9*, P853-858.

Jazwinska, A., & Sallin, P. (2015). Regeneration versus scarring in vertebrate appendages and heart. *Journal of Pathology, 238*, 233-246.

Kawakami, A. (2010). Stem cell system in tissue regeneration in fish. *Development Growth and Differentiation, 52*, 77-87.

Lozito, T. P., & Tuan, R. S. (2016). Lizard tail regeneration as an instructive model of enchanced healing capabilities in an adult amniote. *Connective Tissue Research, 26*, 1-10.

Maden, M., & Varholick, J. A. (2020). Model systems for regeneration: the spiny mouse, *Acomys cahirinus*. *Development, 147*, dev167718.

Marcucci, E. (1930). Il potere rigenerativo degli arti nei rettili. *Archivio Zoologico Italiano, 14*, 227-260.

McCusker, C., Bryant, S. V., & Gardiner, D. M. (2015). The axolotl limb blastema: Cellular and molecular mechanism driving blastema formation and limb regeneration in tetrapods. *Regeneration, 2*, 2–71.

Meenaski, J., Jayaraman, V., Ramakrishnan, K. M., & Babu, M. (2005). Ultrastructural

differentiation of abnormal scars. *Annals of Burns and Fire Disaster, 18*, 83-88.

Mescher, A. L., & Neff, A. W. (2006). Limb regeneration in amphibians: immunological considerations. *Science World Journal, 6* (S1), 1-11.

Mescher, A. L., Neff, A. W., & King, M. W. (2016). Inflammation and immunity in organ regeneration. *Developmental and Comparative Immunology, 66*, 98–110.

Mizel, M. (1968). Limb regeneration: induction in the newborn opossum. *Science (New Series), 161*, 283-286.

Mizel, M., & Isaacs, J. J. (1970). Induced regeneration of hindlimbs in the newborn opossum. *American Zoologist, 10*, 141-155.

Neufeld, D. A., & Zhao, W. (1993). Phalangeal regrowth in rodents: post-amputational bone regrowth depends upon the level of amputation. *Progress in Clinical and Biological Research, 383*, 243-252.

Pritchard, J. J., & Ruzicka, A. J. (1950). Comparison of fracture repair in the frog, lizard and rat. *Journal of Anatomy 84*, 236–262

Richards, C. M., Carlson, B. M., & Rogers, S. L. (1975). Regeneration of digits and forelimbs in the Kenyan red frog *Hyperolius viridiflavus ferniquei*. *Journal of Morphology, 146*, 431-446.

Rinkevich, Y., Maan, Z. N., Walmsley, G. G., & Sen, S. K (2015). Injuries to appendage extremities and digit tips: a clinical and cellular update. *Developmental Dynamics, 244*, 641-650.

Scala, C., Cenacchi, G., Ferrari, C., Pasquinelli, G., Preda, P., & Manara, G. C. (1992). A new acrylic resin formulation: A useful tool for histological, ultrastructural, and immunocytochemical investigations. *Journal of Histochemistry and Cytochemistry*, *40*, 1799-1804.

Scharf, A. (1961). Experiments on regenerating rat digits. *Growth 25*, 7-23.

Schultz, J., Schrottner, P., Leupold, S., Dragu, A., Submann, S., Haase, M., & Fitze, G. (2018). Conservative treatment of fingertip injuries in children- first experiences with a novel silicone finger cap that enables wound fluid analysis. *GMS Interdisciplinary Plastic and Reconstructive Surgery DGPW, 7*, 1-12.

Smith, A. R. (1978). Digit regeneration in the amphibian- *Triturus cristatus*. *Journal of Embryology and Experimental Morphology, 44*, 105-112.

Wu, P, Alibardi, L., Chuong, C. M. (2014). Lizard scale regeneration and development: a model system to analyze mechanisms of skin appendages morphogenesis in amniotes. *Regeneration, 1*: 15-26.

Yang, J. A., Kim, E. S., Kwon, J. H., Kim, H., Shin, J. H., Yun, S. H., Choi, K. Y., & Hahn, S. K. (2012). Transdermal delivery of hyaluronic acid-human growth hormone conjugate.

Biomaterials, 33, 5947-5954.

Zaraisky, A. G., Araslanova, K. R., Shitikov, A. D., & Tereshina, M. B. (2024). Loss of the ability to regenerate body appendages in vertebrates: from side effects of evolutionary innovations to gene loss. *Biological Review of the Cambridge Philosophical Society,* doi 10.1111/brv.13102.

Zhao, W., & Neufeld, D. A. (1995). Bone regrowth in young mice stimulated by nail organ. *Journal of Experimental Zoology, 271*, 155-159.